International Food Research Journal 26(5): 1417-1426 (October 2019)

Journal homepage: *http://www.ifrj.upm.edu.my*

Virtual screening and molecular docking for exploring ACE inhibitory peptides in *Larimichthys crocea* nebulin protein

[1]Yu, Z., [1]Wu, S., [1*]Zhao, W., [2]Ding, L., [1]Li, J. and [3]Liu, J.

[1]*College of Food Science and Engineering, Bohai University, Jinzhou 121013, P.R. China*
[2]*College of Food Science and Engineering, Northwest A&F University, Yangling 712100, P.R. China*
[3]*Laboratory of Nutrition and Functional Food, Jilin University, Changchun 130062, P.R. China*

Article history

Received: 28 February, 2019
Received in revised form: 3 May, 2019
Accepted: 14 June, 2019

Keywords

Nebulin
ACE inhibitory peptide
Molecular docking
Molecular dynamics studies
Pharmacophore modelling

Abstract

Larimichthys crocea nebulin protein was selected to explore novel angiotensin-converting enzyme (ACE) inhibitory peptides. After *in silico* gastrointestinal proteolysis using pepsin, trypsin and chymotrypsin, several tripeptides were obtained. Then, the cytotoxicity, solubility, bioactivity probability, and adsorption, distribution, metabolism and excretion (ADME) properties of the tripeptides were predicted using online prediction tools. Molecular docking was performed to screen the tightly bound peptides to investigate the interactions between ACE and the novel tripeptides. Finally, potent ACE inhibitory tripeptides were used to explore the active pharmacophores. These results suggested that the tripeptide HGR (His-Gly-Arg) exhibited effective ACE inhibitory activity, with an IC_{50} value of 106 ± 1.35 μM. The HGR-ACE complex is stabilised by 14 hydrogen bonds, one attractive charge, and one pi-alkyl interaction. In addition, HGR made contact with the major residues of ACE, i.e., His353, Glu384, Ala354, His513, Tyr523, and Lys511. Furthermore, hydrogen bond acceptors and hydrophobicity are inevitably the most important active features of ACE inhibitory tripeptides, especially hydrogen bond acceptors.

Introduction

There has been increased interest in food-derived bioactive peptides because of their ability to prevent chronic diseases (Hall *et al*., 2018), i.e., cardiovascular diseases, cancers, chronic respiratory diseases and diabetes. Angiotensin converting enzyme (ACE) inhibitory peptide is a heavily researched bioactive peptide, and ACE inhibitory peptides have been identified in a wide variety of foods, such as *Tetradesmus obliquus* green microalgae (Montone *et al*., 2018), casein (Tu *et al*., 2018a), egg white protein (Abeyrathne *et al*., 2018), Chlorella vulgaris (Xie *et al*., 2018), and wheat (*Triticum aestivum*) (Garg *et al*., 2018). Recently, many studies have also highlighted the ACE inhibitory activity of fish protein hydrolysates (Zamora-Sillero *et al*., 2018). The large yellow croaker (*Larimichthys crocea*) is an important marine fish in the world aquaculture industry (Yu *et al*., 2017), and is widely cultured in China (Wang *et al*., 2017a). However, few studies have focused on *L. crocea* as a source of ACE inhibitory peptides.

To date, the generation of ACE inhibitory peptides is based on enzymatic hydrolysis, which is the effective and classical method (Lee and Hur, 2017; Zamora-Sillero *et al*., 2018). Gastrointestinal enzymes (i.e., pepsin, trypsin, and chymotrypsin) have commonly been applied for the enzymatic digestion of proteins (Grootaert *et al*., 2017). Peptides released by *in vitro* gastrointestinal digestion may have relative stability in the gastrointestinal tract. However, this classical method to obtain protein hydrolysates with bioactive properties has a number of drawbacks (Nongonierma and Fitzgerald, 2018). The process used to isolate and purify peptides from enzymatic hydrolysate is generally time-consuming and expensive (Vercruysse *et al*., 2008). Moreover, it is difficult to obtain high purity and highly active peptides from complex mixtures of various peptides (Han *et al*., 2018).

Targeted screening methods may have advantages when compared with the classical method, based on *in silico* tools (i.e., ExPASy PeptideCutter (Gasteiger *et al*., 2003), ToxinPred (Gupta *et al*.,

*Corresponding author.
Email: zhaowenzhu777@163.com

2013), PeptideRanker (Mooney *et al*., 2012), peptide property calculator, admetSAR (Cheng *et al*., 2012) and databases. In fact, several studies have linked a wide range of targeted screening methods that were successful in identifying novel bioactive peptides from food proteins (Wang *et al*., 2017b; Agirbasli and Cavas, 2017; Tu *et al*., 2018a).

Based on the above rationale, the aim of the present work was to identify novel ACE inhibitory peptides from *L. crocea* nebulin protein using *in silico* gastrointestinal digestion and virtual screening methods. Furthermore, molecular docking was employed to investigate the interactions between ACE and the novel peptides. In addition, the 3D quantitative structure-activity relationship (QSAR) pharmacophore model was employed to study the relationship between the primary structure and the activity of ACE inhibitory peptides and assist in further study to identify ACE inhibitory peptides.

Materials and methods

Materials and reagents

ACE (protease from rabbit lung), hippuryl-histidyl-leucine (HHL) and hippuric acid were purchased from Sigma-Aldrich Co. (St. Louis, MO, USA). Acetonitrile, methanol and trifluoroacetic acid were purchased from Fisher Scientific Co. (Waltham, MA, USA) and were of chromatographic grade. All the other reagents and chemicals used were of analytical grade. The synthetic peptides were provided by Shanghai Top Peptide Biological Technology Corporation (Shanghai, China).

In silico gastrointestinal digestion of Larimichthys crocea nebulin protein

The *L. crocea* nebulin protein sequence (NCBI accession number KKF11904.1) was subjected to simulated proteolysis by using three typical digestive proteases: pepsin (EC 3.4.23.1), trypsin (EC 3.4.21.4), and chymotrypsin (EC 3.4.21.1). The *in silico* digestion was carried out using the online program ExPASy PeptideCutter (http://web.expasy.org/peptide_cutter/). Numbers of peptides would be released, and then, tripeptides were selected and compared with known ACE-inhibitory peptides using the BIOPEP (http://www.uwm.edu.pl/biochemia/index.php/en/biopep) and AHTPDB (http://crdd.osdd.net/raghava/ahtpdb/) programs.

Toxicity, solubility, bioactivity, and adsorption, distribution, metabolism and excretion (ADME) property prediction

The potential toxicity of the unknown tripeptide was analysed according to its important physicochemical properties by using the online tool ToxinPred (http://crdd.osdd.net/raghava//toxinpred/) (Gupta *et al*., 2013). The solubility was estimated by using the peptide property calculator http://www.innovagen.com (Lafarga *et al*., 2015). In addition, PeptideRanker (http://bioware.ucd.ie/~compass/biowareweb/Server_pages/peptideranker.php) was used to predict the bioactivity of the tripeptides, and the online tool admetSAR (http://lmmd.ecust.edu.cn/admetsar1/) was applied to predict the ADME properties of the tripeptides, i.e., human intestinal absorption (HIA), Caco-2 cell permeability, and metabolism parameters.

Molecular docking and analysis of the interactions

The crystal structure of human ACE complexing with lisinopril (1O86.pdb) obtained from the Protein Data Bank (http://www.rcsb.org/) was used as the target to screen tripeptides strongly bound with ACE. The molecular docking procedure was carried out by using the CDOCKER protocol of Discovery Studio (DS) 2017 Client software. The structure of the enzyme was ascertained by removing water and adding hydrogen atoms (Pan *et al*., 2012). The docking runs were carried out with coordinates x: 41.2073, y: 33.9431, and z: 46.5201 with a radius of 9.

ACE inhibitory activity assay

The assay of *in vitro* ACE inhibitory activity was performed by the reversed phase high-performance liquid chromatography (RP-HPLC) method described by Yu *et al*. (2012).

Pharmacophore model construction and validation

To build the 3D QSAR pharmacophore hypotheses, 28 ACE inhibitory tripeptides collected from AHTPDB (database of antihypertensive peptides) with known IC_{50} values covering a range of four orders magnitude were used. All 3D structures of the tripeptides were built using the Discovery Studio 2017 R2 client, and the activity uncertainty of those tripeptides was set to 1.5. The 3D QSAR Pharmacophore Generation module of the Discovery Studio 2017 R2 client was employed to generate and validate the pharmacophore model. Chemical features including hydrogen bond acceptor (HBA), hydrogen bond donor (HBD), hydrophobic (HYD), hydrophobic_aromatic (HA), and positive ionisable (PI) were given parameters from a minimum of 1 to a maximum of 5. Other default parameters were used.

Results and discussion

Predictions of toxicity, bioactivity, solubility, and ADME properties for tripeptides

Following *in silico* gastrointestinal digestion, 168 unreported tripeptide sequences were generated and selected for the toxicity, bioactivity, solubility, and ADME properties prediction. Molecular weight and size are taken as important physicochemical properties affecting the bioactive properties of the peptides. Moreover, small peptides are considered safe (Garg *et al*., 2018). Some studies have indicated that the shorter the peptide chain, the easier it is for the peptide to interact with ACE active sites (Lin *et al*., 2017). Thus, in the present work, tripeptides with reasonable molecular weight and absorption properties were selected.

The results showed that all of them were non-toxic, along with all the important physicochemical properties they possessed. Tripeptides AGF, QGF, GQW, GNF, GSF, TMF, LMM, GML, GTW, AAW, AAF, LGC, ECF, SNW, HNW, YPY, HQW, AML, ICL, GLR, AMY, EGF, FDN, LIM, HMY, MDY, GDL, AGY, GHY, SGR, HGR, and GQL with

Table 1. Calculation results of *in silico* bioactivity, toxicity, solubility, ADME properties and docking score of tripeptides released from *Larimichthys crocea* nebulin protein.

Peptide sequence	Peptide ranker	Toxicity	Solubility	ADME properties predictions		–CDOCKER-INTERACTION-energy (kcal/mol)
				Human intestinal absorption	Caco-2 permeability	
AGF	0.96	non-toxic	poor	—	—	—
QGF	0.94	non-toxic	poor	—	—	—
GQW	0.94	non-toxic	poor	—	—	—
GNF	0.94	non-toxic	poor	—	—	—
GSF	0.93	non-toxic	poor	—	—	—
TMF	0.91	non-toxic	poor	—	—	—
LMM	0.91	non-toxic	poor	—	—	—
GML	0.91	non-toxic	poor	—	—	—
GTW	0.87	non-toxic	poor	—	—	—
AAW	0.85	non-toxic	poor	—	—	—
AAF	0.83	non-toxic	poor	—	—	—
LGC	0.82	non-toxic	poor	—	—	—
ECF	0.8	non-toxic	good	HIA-	Caco2-	—
SNW	0.78	non-toxic	poor	—	—	—
HNW	0.77	non-toxic	poor	—	—	—
YPY	0.74	non-toxic	poor	—	—	—
HQW	0.74	non-toxic	poor	—	—	—
AML	0.74	non-toxic	poor	—	—	—
ICL	0.71	non-toxic	poor	—	—	—
GLR	0.71	non-toxic	good	HIA-	Caco2-	—
AMY	0.7	non-toxic	poor	—	—	—
EGF	0.69	non-toxic	good	HIA+	Caco2-	90.8416
FDN	0.68	non-toxic	good	HIA-	Caco2-	—
LIM	0.64	non-toxic	poor	—	—	—
HMY	0.64	non-toxic	poor	—	—	—
MDY	0.59	non-toxic	good	HIA+	Caco2-	83.4035
GDL	0.55	non-toxic	good	HIA+	Caco2-	80.8434
AGY	0.54	non-toxic	poor	—	—	—
GHY	0.53	non-toxic	poor	—	—	—
VDF	0.51	non-toxic	good	HIA-	Caco2-	—
SGR	0.51	non-toxic	good	HIA-	Caco2-	—
HGR	0.51	non-toxic	good	HIA+	Caco2-	92.4782
GQL	0.5	non-toxic	poor	—	—	—

corresponding peptide scores over the 0.5 threshold were labelled as bioactive in PeptideRanker and then selected for solubility prediction. Eight tripeptides (ECF, GLR, EGF, FDN, MDY, GDL, SGR, and HGR) showed satisfactory water solubility, and others showed poor water solubility. The ADME properties of a molecule were all impacted by water solubility (Cheng *et al*., 2003). Soluble tripeptides can be absorbed across the intestinal barrier to reach the target organ or tissue. Thus, tripeptides ECF, GLR, EGF, FDN, MDY, GDL, VDF, SGR, and HGR were selected for determination of ADME properties prediction.

Analysing the results from Table 1, peptides EGF, MDY, GDL, and HGR were labelled as HIA+, and the peptides ECF, GLR, FDN, VDF, and SGR were labelled as HIA-, which indicated that the HIA% of EGF, MDY, GDL, and HGR were more than 30%. On the contrary, the HIA% of ECF, GLR, FDN, VDF, and SGR were less than 30% (Shen *et al*., 2010). Moreover, all of the tripeptides were not CYP450 inhibitors, which indicate that there are less drug-drug interactions in the course of metabolism. Based on the above rationale, tripeptides EGF, MDY, GDL, and HGR passed the ADMET filter and were chosen for further study.

Molecular docking

Molecular docking between ACE and the tripeptides (i.e., EGF, MDY, GDL, and HGR) was performed to screen the tightly bonded tripeptides and explore the molecular mechanism using the CDOOCKER program, a flexible docking tool of Discovery Studio 2017 software.

The best docking positions of tripeptides HGR, EGF, GDL, and MDY, are shown in Figure 2 with CDOCKER-INTERACTION-ENERGY values of -92.4782, -90.8416, -80.8434, and -83.4035 kcal/mol, respectively. A lower 'CDOCKER-INTERACTION-Energy' score denotes a more favourable binding. Thus, tripeptide HGR and EGF showed higher affinity than GDL and MDY, which indicated that HGR and EGF may exert higher ACE inhibition than the GDL and MDY.

Figure 1a shows that the MDY–ACE complex is stabilised by a total of 13 hydrogen bonds, including six conventional hydrogen bonds (Glu162, Ala354, Gln281, and Tyr520), five carbon-hydrogen bonds (His353, His383, and His513), and two salt bridges (Glu384 and Lys511). Moreover, the residues His387, Val380, and Ala354 of ACE formed three pi-alkyl interactions with MDY. Additionally, a pi-pi T-shaped interaction was involved with the residue His353.

Figure 1b shows that the GDL–ACE complex is stabilised by a total of nine hydrogen bonds, including three conventional hydrogen bonds (Ala354 and Gln281), three carbon-hydrogen bonds (Tyr523 and His513), one pi-donor hydrogen bond (His353), and two salt bridges (Glu162 and His353). Moreover, the residues Lys511 and Zn701 of ACE formed two attractive charges with GDL. Additionally, the residues His353 and Phe512 of ACE formed two pi-alkyl interactions with GDL, and the residue Val518 formed an alkyl interaction with GDL.

Figure 1c shows that the HGR–ACE complex is stabilised by a total of 14 hydrogen bonds, including six conventional hydrogen bonds (His353, Ala354, Asp377, and Lys511), five carbon-hydrogen bonds (His353, Glu376, Tyr523, and His513), and three salt bridges (Glu384, Lys511, and Glu162). Moreover, the residues Asp377 of ACE formed an attractive charge with HGR. Additionally, the residue Val518 formed a pi-alkyl interaction with HGR.

Figure 1d shows that the EGF–ACE complex is stabilised by a total of seven hydrogen bonds, including three conventional hydrogen bonds (Ala354, Gln281, and Lys511), two carbon-hydrogen bonds (His513 and His353), and two salt bridges (Glu384 and Lys511). Moreover, the residue Trp279 of ACE formed a pi-pi T-shaped interaction with EGF. Additionally, the residue Zn701 formed an attractive charge with EGF.

There are a total of 13, nine, 14, and seven hydrogen bonds that contain nine, six, nine, and six types of ACE residues that form hydrogen bonds with MDY, GDL, HGR, and EGF, respectively. The ACE-tripeptide complex can be stabilised through hydrogen bond interactions, and the peptide-induced inhibition of ACE activity would be promoted through hydrogen bond interactions (Tu *et al*., 2018b).

The real interactions between ACE and the drugs are essential to screen potent ACE inhibitory peptides (Ke *et al*., 2017). Thus, the interactions of ten drugs, i.e., captopril, lisinopril, enalapril, fosinopril, benazepril, quinapril, cilazapril, ramipril, moexipril, and perindopril (shown in Table 2) with ACE were analysed, and the value of CDOCKER-INTERACTION-ENERGY was -70.4426, -40.7795, -57.182, -74.2439, -60.0918, -68.7201, -63.9904, -62.5964, -73.9554, and -66.0633 kcal/mol, respectively. The results (shown in Table 2) demonstrated that more than five drugs could interact with ACE at the residues i.e., His353, Glu384, Ala354, His513, Val380, Tyr523, His383, Tyr520, Lys511, Zn701, Ser355, and Val518. Therefore, those residues should play an essential role in ACE binding.

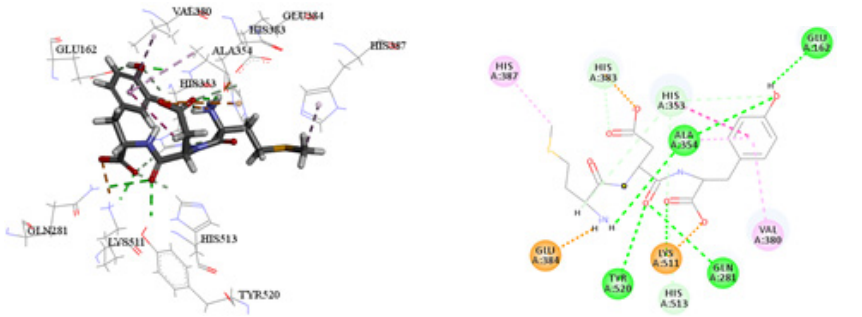

(a)

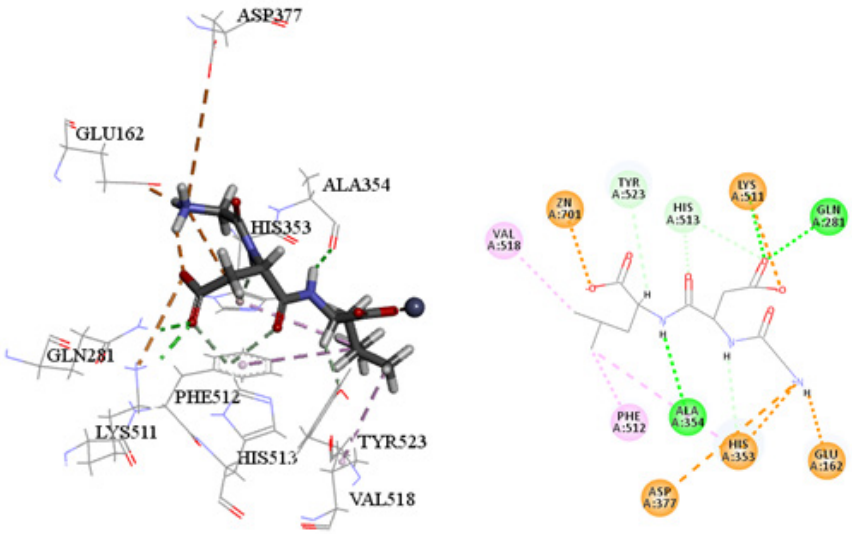

(b)

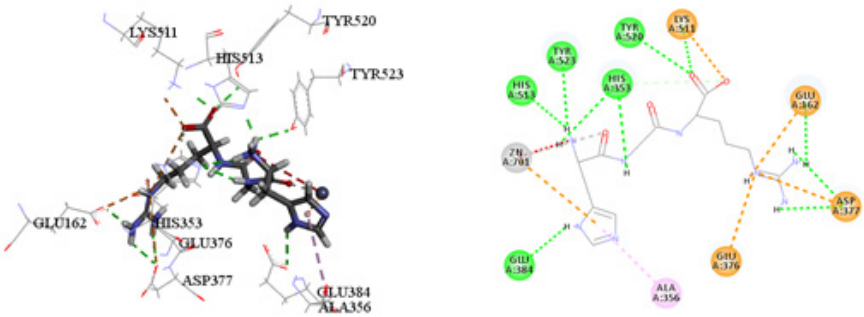

(c)

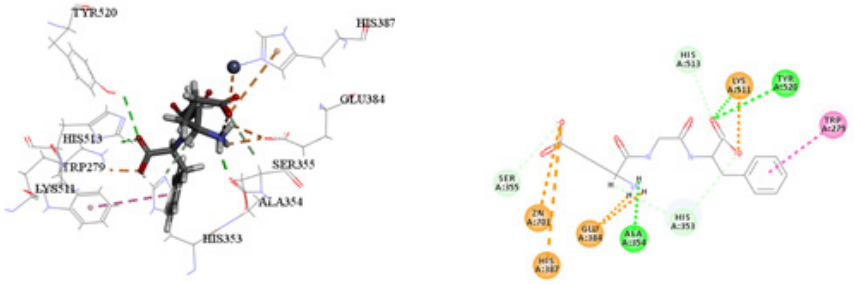

(d)

Figure 1. Binding pose and molecular interactions of the tripeptides MDY (a), GDL (b), HGR (c) and EGF (d) into the active site of ACE, where green colour represents hydrogen bond, orange colour represents salt bridge, attractive charge and pi-anion, pink colour represents pi-pi t-shaped, alkyl, and pi-alkyl, red colour represents unfavourable positive-positive, and grey colour represents metal-acceptor.

Table 2. Interactions of captopril, lisinopril and enalapril derivatives with ACE (PDB ID: 1O86) with their bond length (Å).

	H-bond interacting residues	Hydrophobic bond interacting residues	Electrostatic bond interacting residues	Metal-Acceptor
Captopril	His383 (2.77 Å)	Tyr523 (4.66 Å) His383 (4.25 Å) His353 (5.18Å)	___	___
Lisinopril	Glu162 (2.40 Å) Glu384 (2.53 Å) Ala354 (2.27 Å) His353 (3.04Å) His513 (2.37Å) (2.82 Å) Lys511 (1.87 Å) Tyr520 (2.15Å) Tyr523 (2.55 Å) (4.58 Å) Gln281 (2.09Å)	His383 (4.62 Å) His387 (5.36 Å)	___	Zn701(2.05 Å)
Enalapril	His513 (2.61Å) (2.42 Å) Lys511 (1.74 Å) Tyr520 (2.29Å) Tyr523 (2.69Å) Glu384 (2.05 Å) Ala354 (2.54 Å)	Tyr523 (4.60 Å) His383 (4.97 Å)	___	Zn701 (2.19 Å)
Fosinopril	Gln281 (2.13 Å) Ala354 (2.29 Å) Ser355 (2.64 Å) Glu411 (2.83 Å) Lys511 (2.40 Å) His513 (2.81 Å)	Ala354 (4.21 Å) His387 (4.57 Å) (4.91 Å) Trp279 (4.68 Å) Val380 (3.85 Å) (4.43Å)	___	___
Benazepril	Lys511 (2.96 Å) (1.73 Å) His353 (2.56 Å) (2.56 Å)	Val379 (4.96 Å) His383 (4.89 Å) Ala354 (5.26 Å) Val380 (4.79Å) (5.03 Å) (4.56Å)	Glu162 (4.03 Å)	___
Quinapril	Gln281 (2.67 Å) Tyr520 (2.17Å) Ala356 (2.27 Å) Glu384 (2.05 Å) Ser355 (3.94 Å) His513 (2.81 Å) His353 (2.72 Å)	Val380 (5.48 Å) Ala354 (5.48 Å) Phe527(4.96 Å) Phe457(4.24 Å) Val518 (4.62 Å) (4.87Å)	___	Zn701 (2.10 Å)
Cilazapril	Ser355 (3.74 Å) Ala356 (2.01 Å) (2.02 Å) Glu384 (2.36 Å) Ala354 (3.05 Å) (4.39 Å) His353 (2.79Å) Tyr523 (2.35 Å)	Phe457(5.19 Å) Val380 (4.45 Å) His353 (5.48Å) Phe512 (5.49 Å) Val518 (2.12 Å) (4.66 Å)	___	___
Ramipril	Glu384 (1.99 Å) Ala356 (2.25 Å) Ser355 (2.91 Å) His353 (3.03 Å) Tyr523 (2.78 Å) His513 (2.74 Å) Tyr520 (1.91 Å)	Phe457(4.07 Å) Phe527(5.14 Å) Val380 (4.71 Å) Phe512 (5.37 Å) Val518 (4.40Å) (4.78 Å)	___	Zn701 (1.92 Å)

Table 2. Cont.

Moexipril	Asn70 (2.62 Å) Ser355 (2.68 Å) (3.90 Å) Ala356 (2.25 Å) Glu384 (2.03 Å) His353 (2.79 Å) His513 (2.77 Å) Tyr520 (1.93 Å)	Val518 (4.69Å) His353 (5.81Å) Val380 (4.76 Å) His383 (1.91 Å) Phe527(5.17 Å)	___	Zn701 (2.10 Å)
Perindopril	Gln281 (2.13 Å) Lys511 (1.97 Å) Tyr520 (2.11Å) Glu384 (2.81 Å) Ala354 (2.50 Å) Ser355 (2.71 Å) His513 (2.64 Å)(2.84 Å) Tyr523 (2.40 Å)	Tyr523 (4.77 Å) Val380 (5.45 Å) His383 (4.28 Å)(4.27 Å) Val518 (4.27Å)	___	___

The lowest docking score was for the tripeptide HGR, which could bind with the major residues of ACE, i.e., His353, Glu384, Ala354, His513, Tyr523, and Lys511. Moreover, tripeptide HGR had the highest number of predicted hydrogen bonds. When compared with EGF, GDL, and MDY, the interactions of HGR with ACE were greater. These results indicate that HGR may have stronger inhibitory potency. Thus, tripeptide HGR was subjected to further ACE-inhibitory activity assay.

In vitro ACE inhibitory activity of tripeptide HGR

The ACE inhibitory activity of synthetic tripeptide HGR was tested using the RP-HPLC method. HGR exhibited ACE inhibitory activity with an IC_{50} value of 106 ± 1.35 µM. The AHTPDB program includes 221 ACE inhibitory tripeptides with known IC_{50} values (Kumar *et al*., 2015), and the IC_{50} values of 79 tripeptides were higher than that of HGR. For example, when compared with tripeptides IPA (IC_{50} value of 141 µM), YVP (IC_{50} value of 200 µM), IPY (IC_{50} value of 206 µM), PYP (IC_{50} value of 220 µM), ILP (IC_{50} value of 270 µM), VLP (IC_{50} value of 320 µM), AVP (IC_{50} value of 340 µM), GKP (IC_{50} value of 352 µM), PLP (IC_{50} value of 430 µM), and AGS (IC_{50} value of 527.9 µM), HGR showed a greater ACE inhibitory activity. Based on the analysis, HGR has satisfactory inhibitory activity, and hierarchical virtual screening was used to further advance the research and development of the nature of ACE inhibitory peptides.

3D QSAR pharmacophore model construction and validation

To determine the common structural features necessary for ACE inhibitory tripeptides, 3D QSAR pharmacophore hypotheses were built on 28 ACE inhibitory tripeptides i.e., IKW (IC_{50} value of 0.21 µM), LGP (IC_{50} value of 0.72 µM), VSV (IC_{50} value of 0.15 µM), MAP (IC_{50} value of 0.8 µM), IQW (IC_{50} value of 1.4 µM), IPP (IC_{50} value of 5 µM), LVY (IC_{50} value of 1.8 µM), LIY (IC_{50} value of 0.82 µM), TVY (IC_{50} value of 15 µM), LAP (IC_{50} value of 3.5 µM), LYP (IC_{50} value of 6.6 µM), YAP (IC_{50} value of 14.73 µM), FQP (IC_{50} value of 12 µM), GLP (IC_{50} value of 1.62 µM), FAL (IC_{50} value of 26.3 µM), IPA (IC_{50} value of 141 µM), PLP (IC_{50} value of 430 µM), ILP (IC_{50} value of 270 µM), IAK (IC_{50} value of 15.7 µM), LHP (IC_{50} value of 3,201 µM), IYP (IC_{50} value of 61 µM), DLP (IC_{50} value of 4.8 µM), YVP (IC_{50} value of 200 µM), AVP (IC_{50} value of 340 µM), YKY (IC_{50} value of 43.5 µM), GEP (IC_{50} value of 3,200 µM), PYK (IC_{50} value of 2,400 µM), and PAP (IC_{50} value of 87 µM) collected from the literature. Ten pharmacophore models were generated that were endowed with four features. Fixed and null costs are two important values that are used to judge the quality of pharmacophore hypotheses (Rampogu *et al*., 2018; Peng *et al*., 2018). The values of fixed and null costs were 83.6296 and 689.48, respectively.

In the present work, Hypo 1 with highest cost difference (Dcost: 418.47), lowest root mean square (RMS: 3.67895), and highest correlation coefficient (r: 0.841501) was selected as the most optimal pharmacophore model (shown in Table 3). The most active tripeptide VSV (IC_{50} value of 0.15 µM) had a fit value of 10.780, whereas the least active LHP (IC_{50} value of 3200 µM) showed a lesser fit value of 8.500. Furthermore, the proposed pharmacophore model was then validated by a test set of 116 tripeptides

Table 3. Calculated parameters for ten pharmacophore hypotheses for ACE inhibitory tripeptides.

Hypo No.	Total cost	Null cost distance	RMSD (Å)	Correlation	Feature elements
1	271.01	418.47	3.6790	0.8415	HBA HBA HYDROPHOBIC HYDROPHOBIC
2	307.85	381.63	4.0497	0.8039	HBA HBA HYDROPHOBIC PosIonizable
3	330.52	358.96	4.2620	0.7798	HBA HBA HBA HYDROPHOBIC
4	335.83	353.65	4.3005	0.7752	HBA HBA HYDROPHOBIC HYDROPHOBIC
5	345.43	344.05	4.3818	0.7654	HBA HBA HYDROPHOBIC HYDROPHOBIC
6	368.14	321.34	4.5902	0.7384	HBA HBA HYDROPHOBAromatic HYDROPHOBIC HYDROPHOBIC
7	386.37	303.11	4.7315	0.7190	HBA HBA HYDROPHOBIC HYDROPHOBIC
8	400.89	288.59	4.8335	0.7042	HBD HYDROPHOBIC HYDROPHOBIC PosIonizable
9	406.19	283.29	4.8748	0.6980	HBD HYDROPHOBIC HYDROPHOBIC PosIonizable
10	423.27	266.21	4.9976	0.6791	HBA HYDROPHOBAromatic HYDROPHOBIC HYDROPHOBIC

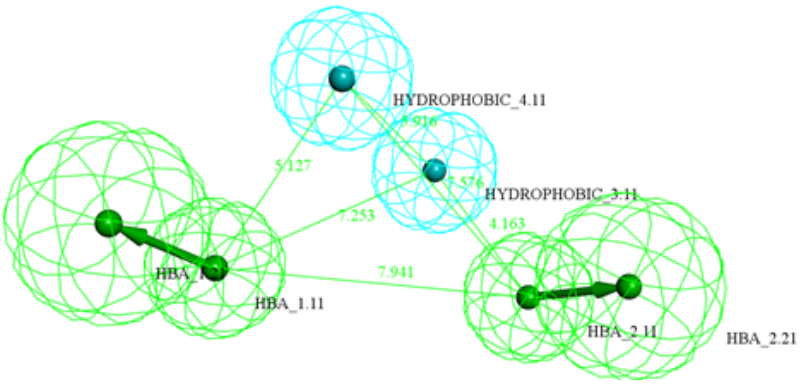

(a)

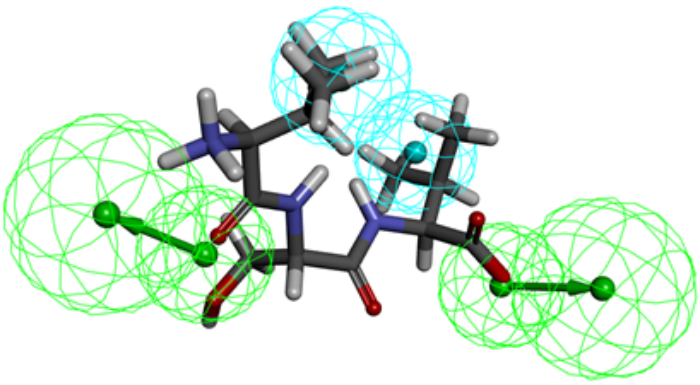

(b)

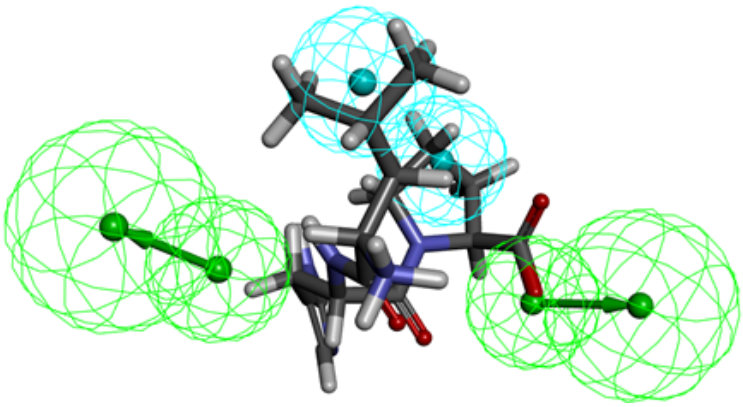

(c)

Figure 2. Pharmacophore model of ACE inhibitory tripeptides generated by 3D QSAR Pharmacophore Generation. (a) The best pharmacophore model was Hypo1 with two hydrogen bond acceptors and two hydrophobic features. The space distances between the features are shown in Å; (b) Hypo1 mapping with the most active tripeptide VSV (IC50 value of 0.15 μM); and (c) Hypo1 mapping with the inactive tripeptide LHP (IC50 value of 3201 μM).

with known activity. The validation results indicated that the regression analysis of experimental and estimated activity of test tripeptides using Hypo 1 gave the highest correlation coefficient (R^2) of 0.117.

Figure 2a shows the Hypo1 chemical features with the inter-feature distances (Å). The best pharmacophore model consists of two HBA (weight: 2.92231), and two HYD (weight: 2.92231) features. As shown in Figure 2b, Hypo1 was very well fitted with the most active tripeptide VSV (IC_{50} value of 0.15 μM) of the training set, including two hydrogen bond acceptors (HBA-1 and HBA-2), and two hydrophobic units (HYD-3.11 and HYD-4.11). As shown in Figure 2c, three pharmacophore features, i.e., HBA-2, HYD-3.11, and HYD-4.11 matched with the most inactive tripeptide LHP (IC_{50} value of 3201 μM). The mapping results corresponded with previous studies, and confirmed that hydrogen bond interactions play an important role in peptide-induced ACE inhibition and that the HBA feature is necessary for ACE inhibitory tripeptides.

Conclusion

In the present work, tripeptide HGR from *L. crocea* nebulin protein was identified using a combination of *in silico* gastrointestinal enzyme digestion and hierarchical virtual screening. Peptide HGR was able to bind with the active site residues of ACE by 14 hydrogen bonds, one attractive charge, and one pi-alkyl interaction. HGR showed significant ACE inhibitory activity *in vitro* with an IC_{50} value of 106 ± 1.35 μM. Furthermore, hydrogen bond interaction was necessary in the peptide-induced ACE inhibition. The HBA feature is essential for ACE inhibitory tripeptide screening.

Acknowledgement

The present work was financially supported by the National Key Research and Development Program of China (2018YFD0400301).

References

Abeyrathne, E. D. N. S., Huang, X. and Ahn, D. U. 2018. Antioxidant, angiotensin-converting enzyme inhibitory activity and other functional properties of egg white proteins and their derived peptides - a review. Poultry Science 97(4): 1462–1468.

Agirbasli, Z. and Cavas, L. 2017. *In silico* evaluation of bioactive peptides from the green algae *Caulerpa*. Journal of Applied Phycology 29(3): 1635–1646.

Cheng, A. and Merz, K. M. 2003. Prediction of aqueous solubility of a diverse set of compounds using quantitative structure - property relationships. Journal of Medicinal Chemistry 46(17): 3572–3680.

Cheng, F., Li, W., Zhou, Y., Shen, J., Wu, Z., Liu, G., … and Tang, Y. 2012. admetSAR: a comprehensive source and free tool for assessment of chemical ADMET properties. Journal of Chemical Information and Modeling 52(11): 3099–3105.

Garg, S., Apostolopoulos, V., Nurgali, K. and Mishra, V. K. 2018. Evaluation of *in silico* approach for prediction of presence of opioid peptides in wheat. Journal of Functional Foods 41: 34–40.

Gasteiger, E., Gattiker, A., Hoogland, C., Ivanyi, I., Appel, R. D. and Bairoch, A. 2003. ExPASy: the proteomics server for in-depth protein knowledge and analysis. Nucleic Acids Research 31(13): 3784–3788.

Grootaert, C., Matthijs, B., Voorspoels, S., Possemiers, S., Smagghe, G. and Van Camp, J. 2017. Egg-derived bioactive peptides with ACE-inhibitory properties: a literature update. Food and Function 8(11): 3847–3855.

Gupta, S., Kapoor, P., Chaudhary, K., Gautam, A., Kumar, R., Open Source Drug Discovery Consortium and Raghava, G. P. 2013. *In silico* approach for predicting toxicity of peptides and proteins. PLoS One 8(9): e73957.

Hall, F., Johnson, P. E. and Liceaga, A. 2018. Effect of enzymatic hydrolysis on bioactive properties and allergenicity of cricket (Gryllodes sigillatus) protein. Food Chemistry 262: 39–47.

Han, J., Tang, S., Li, Y., Bao, W., Wan, H., Lu, C., ... and Su, X. 2018. *In silico* analysis and in vivo tests of the tuna dark muscle hydrolysate anti-oxidation effect. Royal Society of Chemistry Advances 8: 14109–14119.

Ke, Z., Su, Z., Zhang, X., Cao, Z., Ding, Y., Cao, L., … and Xiao, W. 2017. Discovery of a potent angiotensin converting enzyme inhibitor via virtual screening. Bioorganic and Medicinal Chemistry Letters 27(16): 3688–3692.

Kumar, R., Chaudhary, K., Sharma, M., Nagpal, G., Chauhan, J. S., Singh, S., … and Raghava, G. P. 2015. AHTPDB: a comprehensive platform for analysis and presentation of antihypertensive peptides. Nucleic Acids Research 43(D1): D956–D962.

Lafarga, T., O'Connor, P. and Hayes, M. 2015. *In silico* methods to identify meat-derived prolyl endopeptidase inhibitors. Food Chemistry 175: 337–343.

Lee, S. Y. and Hur, S. J. 2017. Antihypertensive peptides from animal products, marine organisms, and plants. Food Chemistry 228: 506–517.

Lin, K., Zhang, L.-W., Han, X. and Cheng, D.-Y. 2017. Novel angiotensin I-converting enzyme inhibitory peptides from protease hydrolysates of Qula casein: Quantitative structure-activity relationship modeling and molecular docking study. Journal of Functional Foods 32: 266–277.

Montone, C. M., Capriotti, A. L., Cavaliere, C., La Barbera, G., Piovesana, S., Zenezini Chiozzi, R. and Laganà, A. 2018. Peptidomic strategy for purification and identification of potential ACE-inhibitory and antioxidant peptides in *Tetradesmus obliquus*

microalgae. Analytical and Bioanalytical Chemistry 410(15): 3573–3586.

Mooney, C., Haslam, N. J., Pollastri, G. and Shields, D. C. 2012. Towards the improved discovery and design of functional peptides: common features of diverse classes permit generalized prediction of bioactivity. PLoS One 7(10): e45012.

Nongonierma, A. B. and Fitzgerald, R. J. 2018. Enhancing bioactive peptide release and identification using targeted enzymatic hydrolysis of milk proteins. Analytical and Bioanalytical Chemistry 410(15): 3407–3423.

Pan, D., Cao, J., Guo, H. and Zhao, B. 2012. Studies on purification and the molecular mechanism of a novel ACE inhibitory peptide from whey protein hydrolysate. Food Chemistry 130(1): 121–126.

Peng, J., Li, Y., Zhou, Y., Zhang, L., Liu, X. and Zuo, Z. 2018. Pharmacophore modeling, molecular docking and molecular dynamics studies on natural products database to discover novel skeleton as non-purine xanthine oxidase inhibitors. Journal of Receptors and Signal Transduction 38(3): 246–255.

Rampogu, S., Son, M., Baek, A., Park, C., Rana, R. M., Zeb, A., ... and Lee, K. W. 2018. Targeting natural compounds against HER2 kinase domain as potential anticancer drugs applying pharmacophore based molecular modelling approaches. Computational Biology and Chemistry 74: 327–338.

Shen, J., Cheng, F., Xu, Y., Li, W. and Tang, Y. 2010. Estimation of ADME properties with substructure pattern recognition. Journal of Chemical Information and Modeling 50(6): 1034–1041.

Tu, M., Liu, H., Zhang, R., Chen, H., Mao, F., Cheng, S., ... and Du, M. 2018a. Analysis and evaluation of the inhibitory mechanism of a novel angiotensin-I-converting enzyme inhibitory peptide derived from casein hydrolysate. Journal of Agricultural and Food Chemistry 66(16): 4139–4144.

Tu, M., Wang, C., Chen, C., Zhang, R., Liu, H., Lu, W., ... and Du, M. 2018b. Identification of a novel ACE-inhibitory peptide from casein and evaluation of the inhibitory mechanisms. Food Chemistry 256: 98–104.

Vercruysse, L., Smagghe, G., Matsui, T. and Van Camp, J. 2008. Purification and identification of an angiotensin I converting enzyme (ACE) inhibitory peptide from the gastrointestinal hydrolysate of the cotton leafworm, *Spodoptera littoralis.* Process Biochemistry 43(8): 900–904.

Wang, P., Zhu, J., Feng, J., He, J., Lou, Y. and Zhou, Q. 2017a. Effects of dietary soy protein concentrate meal on growth, immunity, enzyme activity and protein metabolism in relation to gene expression in large yellow croaker *Larimichthys crocea*. Aquaculture 477: 15–22.

Wang, T.-Y., Hsieh, C.-H., Hung, C.-C., Jao, C.-L., Lin, P.-Y., Hsieh, Y.-L. and Hsu, K.-C. 2017b. A study to evaluate the potential of an *in silico* approach for predicting dipeptidyl peptidase-IV inhibitory activity *in vitro* of protein hydrolysates. Food Chemistry 234: 431–438.

Xie, J., Chen, X., Wu, J., Zhang, Y., Zhou, Y., Zhang, L., ... and Wei, D. 2018. Antihypertensive effects, molecular docking study and isothermal titration calorimetry assay of the angiotensin I-converting enzyme inhibitory peptides from *Chlorella vulgaris.* Journal of Agricultural and Food Chemistry 66(6): 1359–1368.

Yu, Y., Gao, Q.-L., Song, Y., Zhang, J.-Y., Li, Z.-B., Li, W., ... and Qi, Y.-X. 2017. High-throughput screening of potential allergens from complex proteins of large yellow croaker (*Larimichthys crocea*) by mass spectrometry. Chinese Journal of Analytical Chemistry 45(5): e1713–e1718.

Yu, Z., Liu, B., Zhao, W., Yin, Y., Liu, J. and Chen, F. 2012. Primary and secondary structure of novel ACE-inhibitory peptides from egg white protein. Food Chemistry 133(2): 315–322.

Zamora-Sillero, J., Gharsallaoui, A. and Prentice, C. 2018. Peptides from fish by-product protein hydrolysates and its functional properties: an overview. Marine Biotechnology 20(2): 118–130.